Original Article

Parachute emergency landing simulation and enhanced composite material characterization for General Aviation aircraft

Gennaro Di Mauro[ID]**, Giuseppe Maurizio Gagliardi, Michele Guida**[ID] **and Francesco Marulo**

Abstract

General Aviation (GA) aircraft crashworthiness of the vehicle when it hits the ground after the parachute deployment is an important issue. The current dynamic emergency landing regulation (CS 23.562) defines the maximum human tolerant accelerations under both vertical and horizontal directions. This article aims to compare two different aircraft configurations: metal low-wing and composite high-wing ones. Both are two-seats and single-engine GA aircraft. The purpose of the analysis is to check whether the seats and restraint systems met human injury tolerance standards and to determine the possible impact on passengers in the cabin space due to shock loads. Finite element analysis of the fuselage sections for both configurations is performed using the commercial LS-Dyna solver. An extensive campaign of experimental tests has been performed on the composite samples for tuning and validating the model and to find the transition from an undamaged up to totally collapsed sample. The material of the composite fuselage has been characterized through experimental tests. The adopted material model has been refined to match with the performed experimental analysis, allowing high-fidelity modeling. A parametric analysis has been performed to determine the optimal impact angle in terms of lumbar injuries and loads transmitted by the seat belt due to aircraft contact with the ground, thereby increasing the level of safety. The investigations carried out may be an important indicator of the design of the parachute system.

Background

Parachutes reduce the vertical fall speed if deployed vertically or increase the drag on the object if deployed horizontally with respect to the ground. These attributes have been used for centuries in different applications of parachutes. Several factors forced parachute technology to advance very rapidly during the last decades. Among them, the aircraft parachute for emergency landing can be mentioned. Pilot Boris Popov created the first commercial plane parachute in 1980. His company, the Ballistic Recovery Systems (BRS), born in Minnesota in 1980, produced the first commercial parachute to be used with light aircraft in 1982. The company also collaborated with Cirrus Aircraft Corporation in 1998 to produce a parachute recovery system for certified commercial aircraft. Cirrus Aircraft Systems were the first to install Popov's parachute in all their aircraft. Since then, these systems have been tested and installed in various light aircraft like Cirrus SR20, Cessna 162, 172, and 182.[1,2]

General aviation (GA) safety remains a challenging issue, as evidenced by the persistently high accidental mortality.[3,4] In previous studies, various factors were associated with lethal outcomes, including flight phase, meteorological conditions, terrain, and pilot skills.[5] Fatal accidents are usually high-energy events due to flight speed, impact force and impact angle. During a fatal impact, deceleration occurs when hitting the ground, resulting in a transfer of force that is often beyond human biomechanics.

Industrial Engineering Department of University of Naples Federico II, Naples, Italy

Corresponding author:
Gennaro Di Mauro, Industrial Engineering Department of University of Naples Federico II, Via Claudio, 21, Naples 80125, Italy.
Email: gennaro.dimauro@unina.it
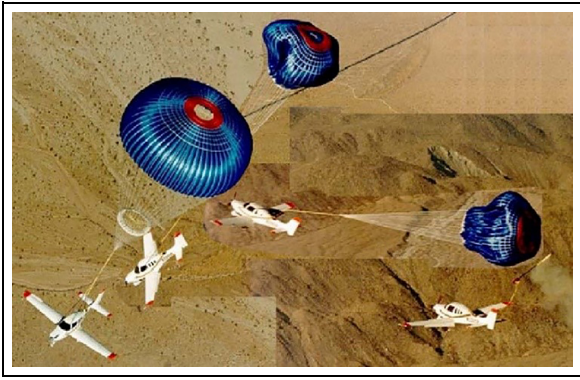
Figure 1. Cirrus SR20 aircraft after the BPRS deployment.[9]

Studies have shown that the speed and elevation angle of an aircraft during impact affects survivability.[6] Efforts to reduce fatalities have focused on pilot training and the implementation of energy-absorbing structures to reduce the transmission of shock forces to the occupants. These efforts include Federal Aviation Administration (FAA) approved pilot safety courses, crash fuselage, shoulder harnesses, energy-absorbing seats and airbags. More recently, Ballistic Parachute Recovery Systems (BPRS) have been installed on GA aircraft to improve survivability in a crash event. The BPRS deployment determines two major operational changes: aircraft descent no longer requires pilot control, and speed is reduced before the impact.[7,8] Nowadays, Cirrus Corporation equips many of its aircraft with this recovery system, the so-called Cirrus Airframe Parachute System (CAPS).[9–11] Experimental tests with the Cirrus SR20 aircraft can be observed in Figure 1. For a detailed study on the design, manufacturing, testing, and operation of parachute recovery systems is provided in Knacke.[12]

A focus of the emergency landing is the crash safety of the vehicle hitting the ground after the parachute deployment. The current regulation CS 23.562[13] for dynamic emergency landing conditions expects the loads not to exceed 680 kg for the lumbar and 794 kg for the shoulder. The purpose of this work is to check that seats and restraint systems meet injury compatibility standards and to determine the potential impact on occupants in the cabin due to shock loads. The main objective is to determine the optimal impact angle in relation to lumbar loads and loads transmitted by seat belts during aircraft contact with the ground, to increase the level of safety. Therefore, the parachute ropes can be properly designed to make the aircraft collide the ground at an optimum elevation angle for passenger safety.

The aim of the article is to perform a comparative study between two different cabin solutions for a GA aircraft, mentioned before. Therefore, it has been necessary to deal with composite material modeling. The design of the structural components with high crashworthiness depends on the crash resistance concept described by Kindervater and Georgi[14] and Guida et al.[15] The crash resistance concept is based on the energy absorption capacity and structural integrity. Nowadays, with reference to the aeronautic field, many kinds of structural components have been realized by composite materials since they are capable to absorb a high amount of impact energy and can guarantee the survival of the passengers.[16]

The behavior of the material under crash loads[17–19] and the contribution of several component of the aircraft structure is very complex. Many concurrent phenomena can affect laminate failure under impact load: fiber breakage,[20–22] delamination,[23] matrix cracking,[24] plastic deformations due to the contact[25] and large displacements,[26,27] damage propagation,[28,29] are some effects that must be considered when a composite structure is impacted.

Impact tests on composite laminates are fundamental to characterize the material in terms of damage tolerance and energy absorbing capabilities[30]: typically, low-velocity impact tests[31–33] are the preferred ones since they can eventually exhibit the above-mentioned phenomena.

Two kinds of impact exist, depending on the velocity of the impactor striking the specimen. Under low-velocity impact loading conditions, the contact time between the projectile and the target is longer. Thus, the entire structure collaborates and allows kinetic energy to be absorbed also at points remote from the impact location.[34,35] Conversely, high-velocity impact loads from light projectiles tend to cause the target response to be more localized, resulting in energy being distributed over a relatively small area. These two different forms of shock loading will produce different degrees of damage and have different consequences on the subsequent bearing capacity of the structure.[36] The crushing phenomenon, the energy absorption mechanisms, and the passengers' injuries were evaluated in the last years in some works proposed in the literature. A very comprehensive study about the FE modeling of the fuselage skin, seats, belts, and beams is detailed in Caputo et al.[37] The energy absorption capability of a full-scale composite fuselage section is detailed in Perfetto et al.[38]

The case study of this work refers to a low-velocity impact load condition since the parachute opening in an emergency landing condition is taken into account. An impact velocity of 9.14 m/s is considered, provided by the requirement, and the scenario defines the best practices for the aircraft cabin design as well as the different behaviors of the material structures that can generate ideas for design thinking.

Finite element analysis

Finite element analysis has been performed to study the behavior of a GA aircraft during an emergency landing. A focus was provided on airframe

crashworthiness issues to define the ultimate loads transferred to passengers. The purpose was to define the optimal elevation angle to minimize the lumbar load and the load transmitted by the seat belt for both aircraft configurations. The following sections describe a preliminary model aimed to investigate the most sensitive parameters of the phenomenon taken into account. Then, two final models have been created to explore the differences lying between them in terms of crashworthiness.

Preliminary simplified model

Initially a simplified model of the aluminum fuselage has been created to have some preliminary results of the problem and to evaluate the feasibility of a one-dummy model to reduce the computational cost. Finite Element analysis of a partial section of the fuselage has been performed using the LS-Dyna software. The model, shown in Figure 2, includes seats, restraints, dummies, and the structural elements that could intercept the trajectory of the passengers during the crash events.

The model consists of:

- Fuselage: in this application, the truss presents two different sections: circular (red) and square
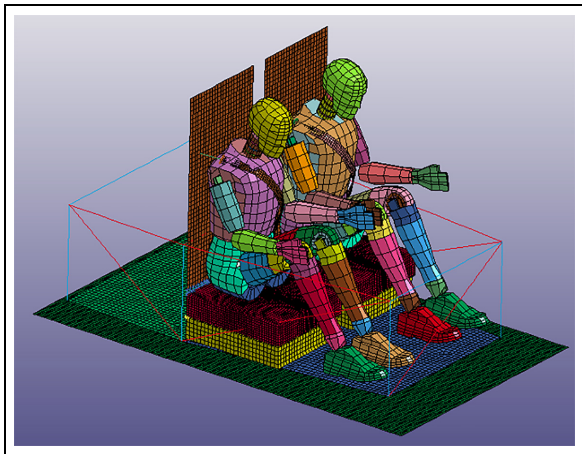
Figure 2. Simplified FE Model of the cabin.

(blue) beams. Then, there is the lower skin in aluminum material to guarantee surface-to-surface contact during the impact.

- Ground: it is considered a rigid plate; in the analysis, it is completely fixed, and the aircraft moves toward it defining contacts.
- Seats: there are two seats modeled as two plates, the first one for the seat and the second one for the back.
- Dummy: two hybrid III dummies have been imported to investigate the human evolution during the impact. Surface-to-surface contact algorithms assigned to model the interaction between the dummies, the cushions, and the structures have been considered. The crash dummy is composed of many parts, joints, and sensors. For the simulations, two different parameters have been considered:
- Lumbar loads transmitted during the emergency landing. The compression force values were measured on junctions between the lumbar and pelvis of the dummies and the load is recorded.
- Loads transmitted in the proximity of the interaction between the belt and the shoulder, where the junction between the shoulder and homer is present.
- Belt: the material is polyester, and this item consists of pelvis belt and lap belt, both presents two attachment points directly connected to the seat structure. The fabric is modeled in the 2D elements and the connection with the structure is enhanced by 1D rigid elements in order to involve several nodes. The load and unload curves of the 1D element connecting the structure and the 3D shells have been taken from experimental data as shown in Figure 3.
- Cushion: the square seat cushions have been realized in Polyurethane DAX26 foam, commonly used in aircraft seats manufacturing, with a density of $38 \, kg/m^3$, and a Young Modulus of $0.5 \, GPa$. The thickness of these components is $100 \, mm$, and the shape adapts to the space available inside the fuselage. It has been implemented in LS-Dyna software using 3D fully integrated elements, and in the Figure 4 its stress-strain
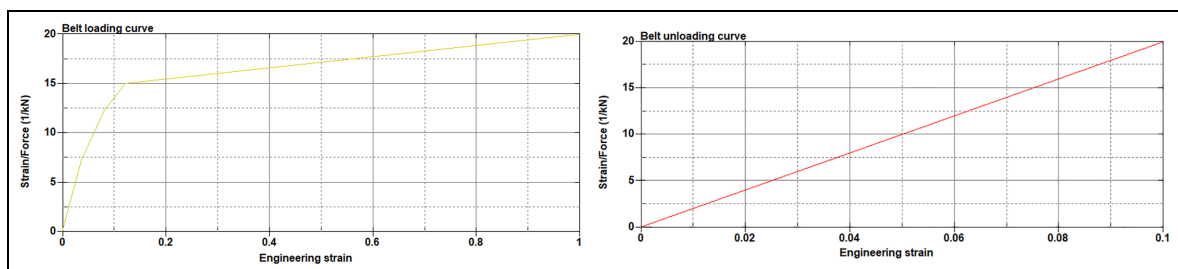
Figure 3. Belt loading/unloading curve.

curve is reported. This material type has been specifically developed for modeling highly compressible low-density foams. The kind of cushion foam utilized is quite soft compared to other foams typically used in aeronautical applications (i.e. DAX55) and it is possible to neglect its initial deformation, as discussed in Russo et al.[39]

The landing gear has not been modeled to be conservative and to account for the possibility that the pilot, in an emergency, forgets to pull out the landing gear.

Low-wing aluminum model

The cabin consists of truss and skin parts. Since it is a low-wing airplane, there are no doors and the upper part of the fuselage presents a large canopy, so pilots can board from above. Only the ceiling beams that carry the glasses were modeled. The glass part of the canopy was not modeled as it is not necessary for this type of analysis since it is not a structural component. The lower part of the fuselage consists of truss and skin parts. In particular, the bottom skin is flat, as for this kind of airplane it is necessary to integrate the cabin and the low wing. The structural part of the
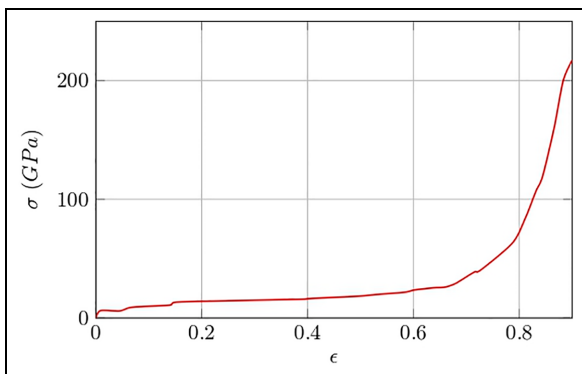
model, without the dummy, is represented in Figure 5(a). Concerning the material model, a 2024 T3 aluminum alloy has been considered, whose characteristics can be found in Guida et al.[17]

High-wing composite model

For composite aircraft, the cabin was modeled using shell elements that represent the centerline of the laminate. The number of integration points was equal to the number of layers through the thickness, resulting in one integration point for each layer. The Belytschko-Tsay failure model has been employed. The seat was mounted on two trusses, an aluminum truss, which was also connected to the rear landing gear, and a composite one. In particular, the last one is an open section beam which allows high deformations and energy absorbing capabilities. In this case, the lower part of the cabin is curved, and a floor is present. Since it is a high-wing configuration, doors and ceilings were considered. The structural part of the model is represented in Figure 5(b). The composite material properties, referred to a fabric ply, are summarized in Table 1. Further details about the mesh and the boundary conditions are provided in Figure 6.

Case study

A sensitivity analysis has been performed for both configurations by varying the impact angle. Since both the aircraft have forward-located engines and propellers, the center of gravity lies quite ahead. At the same time, it is not possible to locate the parachute attachment too forward. Consequently, the airplane has a negative elevation angle during the impact on the ground. Properly designing the parachute strips, it is only possible to make minor changes in the impact angle. Thus, it has been evaluated the feasibility of a negative elevation angle between 9° and 21°. For the numerical analyses also two extreme conditions (0° and 40°) were tested to represent the
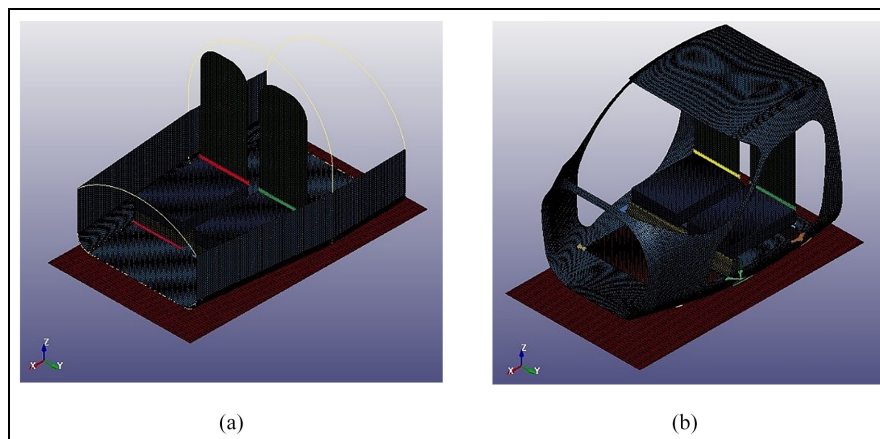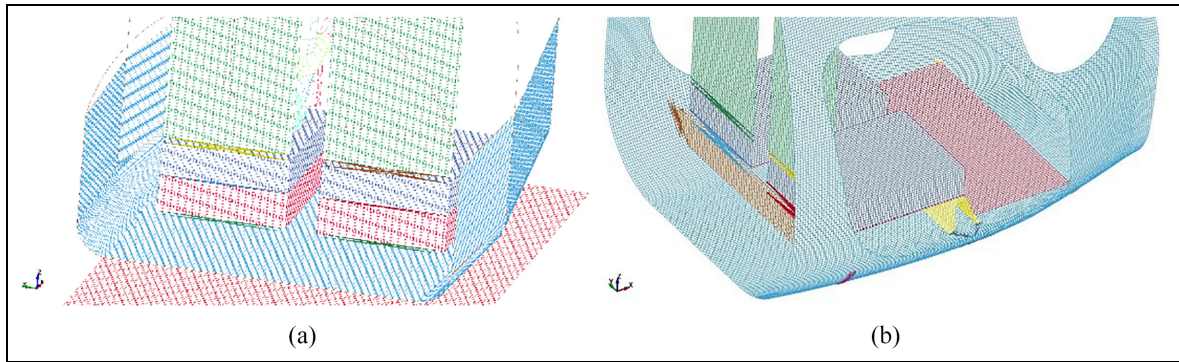

Figure 4. Stress-strain curve of the cushion foam.

(a)   (b)

**Figure 5.** Low-wing metallic (a) and high-wing composite (b) FE Models.

Figure 6. Mesh and boundary conditions detail of the low-wing metallic (a) and high-wing composite (b) airplane.

Table 1. Table of the composite material adopted for the high-wing fuselage configuration.

Characteristic	Value	Unit of measurement
E_A	55	GPa
E_B	55	GPa
v_{AB}	0.4	-
G_{AB}	4.2	GPa
G_{BC}	2.9	GPa
G_{AC}	2.9	GPa
ρ	1.6	kg/mm^3
h	0.15	mm
S_C	0.075	GPa
X_T	0.18	GPa
Y_T	0.075	GPa
Y_C	0.075	GPa
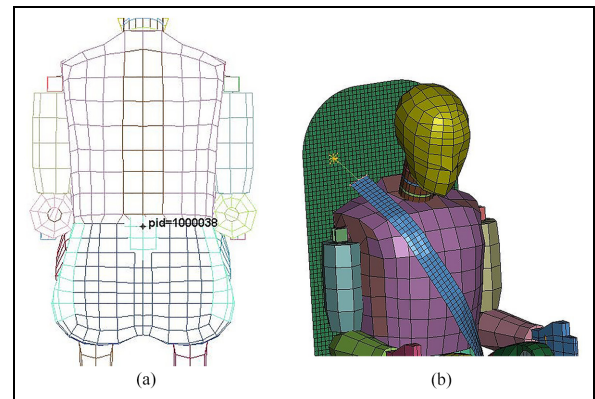
Figure 7. Locations of the dummy in which the loads are evaluated: (a) lumbar point and (b) shoulder point.

behavior of the aircraft in two extreme conditions. From the numerical model point of view, the variation in the impact angle has been simulated by inserting the two vertical and horizontal components of the velocity vector. The magnitude of the velocity vector is the same for all the tests: 30 ft/s (9.14 m/s). Only its direction has been changed to properly consider the impact angle.

The crash dummy is composed of many parts, joints, and sensors. In the current simulations two different parameters have been considered:

- The lumbar loads transmitted during the emergency landing. The compression force values were measured on junctions between the lumbar and pelvis of the dummies (Figure 7(a)) and the load has been recorded.
- The second parameter is the load transmitted in the proximity of the interaction between the belt and the shoulder (Figure 7(b)), where the junction between the shoulder and homer is present.

Results

The purpose of this study was to investigate the safety differences in the use of aluminum and fiber-

reinforced composite materials for the fuselage of light aircraft under a crash landing. The overall safety zone of the carbon fiber reinforced composite is higher than that of the aluminum cabin. Aircraft are not comparable because carbon fiber is applied in high-wing configuration, while aluminum alloy is considered in low-wing configuration, but for the samples in this study the impact velocity is the same and the kinetic energy has the same trend, decreases gradually and remains stable after impact, while the internal energy increases with time, and ultimately the total energy is conserved.

Simulation

A classical simulation is represented in Figure 8. At the first instant (Figure 8(a)), there is still clearance between the vehicle and the ground, and the model has an initial velocity of 9.14 m/s. At a subsequent instant (Figure 8(b)), the cabin has its first impact on the ground. Some deformations appear in the skin of the fuselage. The dummy is unmoved since the acceleration is not yet transmitted. At the third represented instant (Figure 8(c)), further deformations in the structure appear and the dummy is moved by the forces of inertia and then it is gradually decelerated.
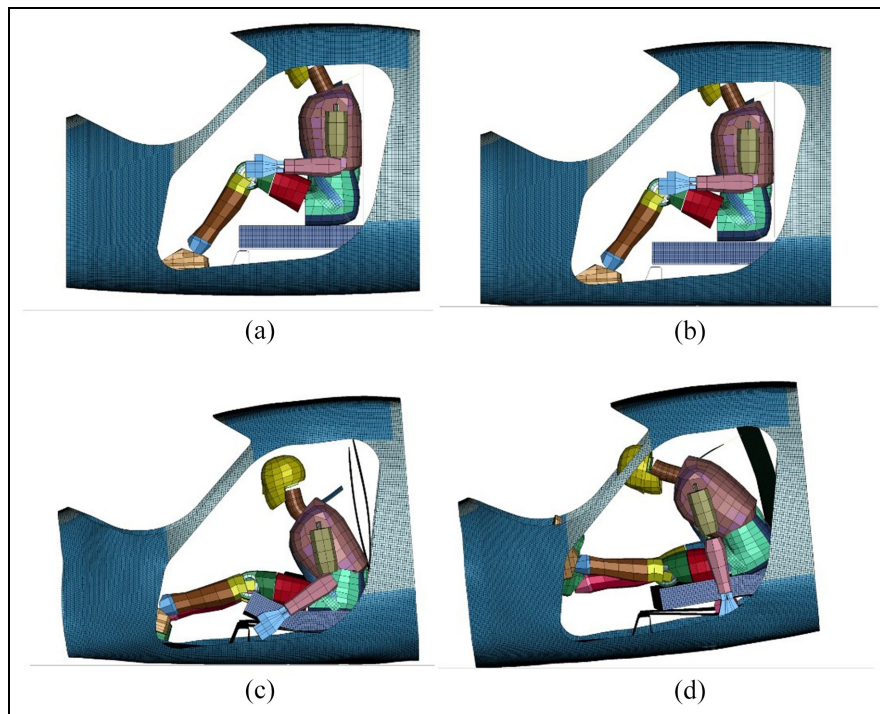
Figure 8. Four significant instants of a typical parachute landing simulation for CF configuration: (a) simulation starts ($t = 0$ ms), (b) first impact ($t = 25$ ms), (c) inertia forces and start of deceleration ($t = 75$ ms), and (d) deceleration and belt action ($t = 100$ ms).

In the final stage (Figure 8(d)), the vehicle is totally decelerated, and the dummy is held by the belt. At this point, evaluations about residual energy were performed. The impact dynamics are quite similar during the contact phases. Differently, the forces involved are different, both the intensity of the force transmitted on the pelvic zone of the dummy and the force on the belt can assume substantially different values. Therefore, the analysis of these two values has been carried out for each angle of impact. If one looks at the fuselage from above (Figure 9) during the crush of the cabin, some cracks and failures of elements are visible, certifying the functioning of the composite material failure mechanism. In any case, the cracks are not very serious and the structural integrity of the entire cabin is not compromised.

Composite material characterization

One of the critical aspects concerning composite materials definition is the lack of constitutive models capable of describing the transition from an undamaged to a progressively damaged material up to its complete collapse of the material.[40–43] In addition, for the actual component, which is the fuselage, the manufacturing process has to be taken into account, together temperature and pressure adopted during the polymerization process. Because of that, an impact test campaign has been conducted to have an experimental validation and tuning of the material model. A portion of the fuselage skin has been tested to obtain enhanced information about the constitutive
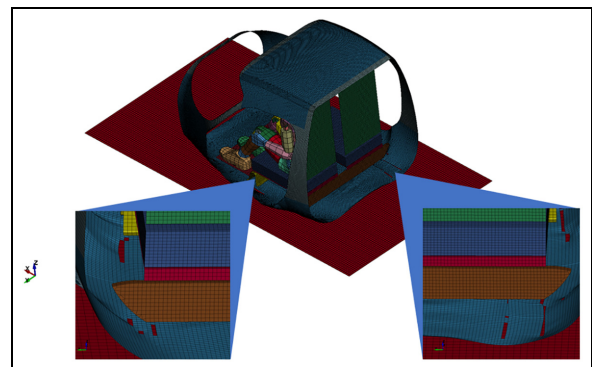

Figure 9. Detail about the failure mechanisms of the CF fuselage floor.

model of the composite material. A drop tower has been adopted to carry out the experimental campaign. It consists of four rectified metal columns fixed on a metallic base. The columns have been characterized by four tracks that allow ensuring the guidance of a falling frame, equipped with eight steel wheels.

The sample on the structure to be tested has been fixed under the dart with the aid of a ground support. It consists of a base on which a metallic frame is fixed. The frame itself is characterized by a rectangular hole, whose dimensions are given by ASTM D7136 requirement,[44] enabling the deflection of the sample subjected to the impact test. To obtain the desired boundary conditions, four clamps are mounted on the ground frame to make it possible to constrain the

sample on the edges. This experimental device is instrumented with a set of sensors that allow to measure various test parameters, in particular the force and the acceleration. A first piezoelectric sensor measures the moveable frame acceleration during its fall, the impact phase and the rebound. A second piezoelectric sensor is used to measure the acceleration on the impacted sample. A piezoelectric force sensor, embedded into the dart itself, allows to obtain the contact force between the dart and the sample. A SCADAS data logger was used for monitoring the outputs in time during the tests. Figure 10 shows the general set-up for the performed tests.

A numerical model of the composite laminate has been created in LS-Dyna software to simulate the test. The composite shell has been modeled in the same way as in the full cabin model. The dart has been modeled as a sphere made of a rigid material. The density of this material has been tuned in such a way to have the same total mass of the impacting apparatus. Thus, the dart force and the acceleration of the plate in the measurement point have been computed and compared with the experimental ones. Figure 11 shows the comparison of the time domain behavior of the force and the acceleration between numerical and experimental results. For the force signal, a filtering operation has been performed to delete high-frequency peaks due to structural vibration and correctly evaluate the force peak. A very good
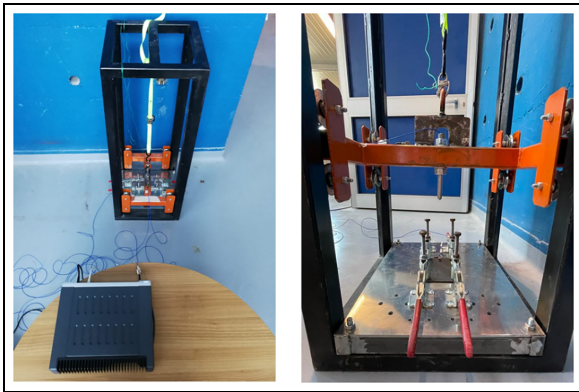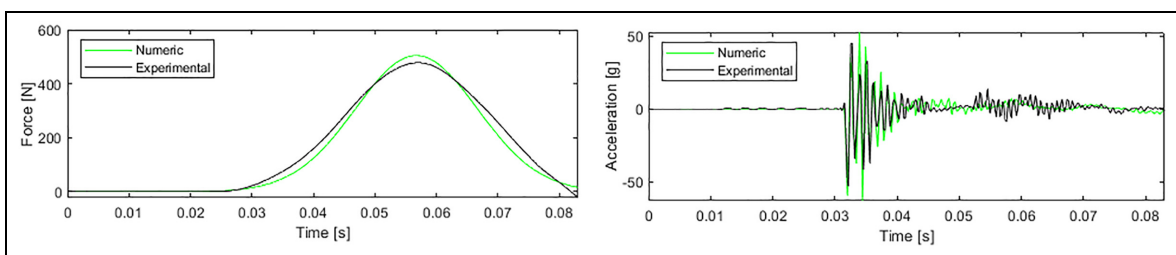
correspondence has been obtained for both signals, resulting in a validation of the numerical model of the material.
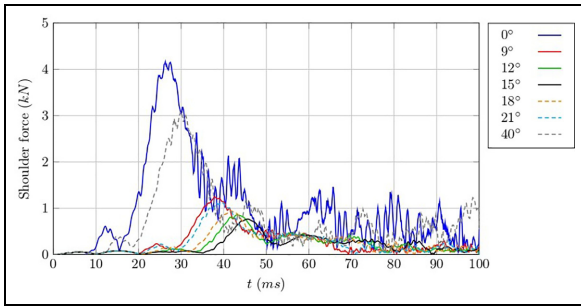
Sensitivity analyses

A sensitivity analysis has been addressed to individuate the optimal impact angle of the two considered vehicles. The angles of interest for this study are contained in the range between 9° and 21°. These values have been obtained through a feasibility analysis based on the center of gravity oscillation and the amount of correction possible with the parachute strips. In addition, two extreme conditions have been considered: 0° and 40°. To simulate the incidence, the velocity vector has been split into two components along the x and z directions.

This work shows that the reduction of compressive forces transmitted to the lumbar of the passenger and the hardness of the seatbelt are two key aspects of crashworthiness assessment. Figure 12 shows a comparison between shoulder forces for all impact angles for the metallic low-wing configuration. As expected, the two extreme conditions were characterized by higher forces.
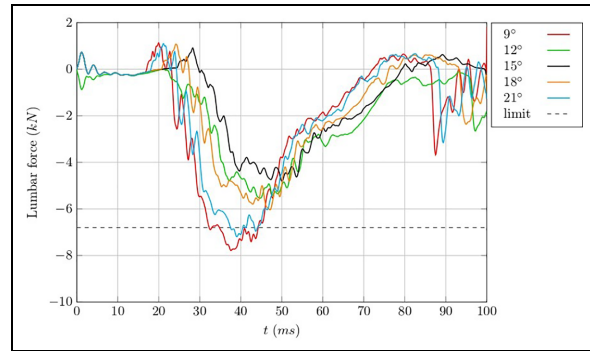
In Figure 13 the same diagram is repeated, removing the extreme conditions, at 0° and 40° impact angles. It allows to study the angle of attack in relation to the peak and duration of the load transferred to the shoulder. All analyzed configurations showed peaks under the limit (7.94 kN). Of all the curves, however, the best condition is obtained at 15°.

For each configuration, a similar approach was considered for the loads transferred to the lumbar region (Figure 14). Focusing on the selected angles (Figure 15), the better condition is obtained at 15°, a value that respects the requirement. Even if the optimal angle is not achieved, the curve is still under the limit. Notice that a correspondence between the optimal angles for shoulder and lumbar loads is obtained. This is because the effect of the horizontal component of the velocity vector gives a small contribution to the loads. The main contribution is still due to the vertical component, as it causes the dummy to move forward and thus the bending of the spinal column, which provides a belt load.
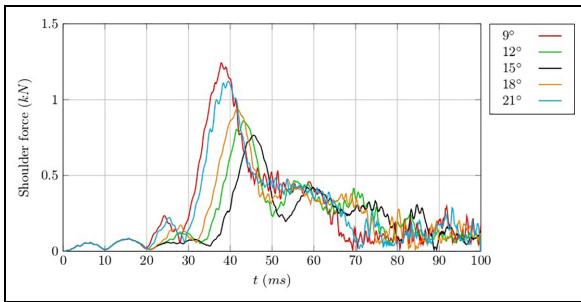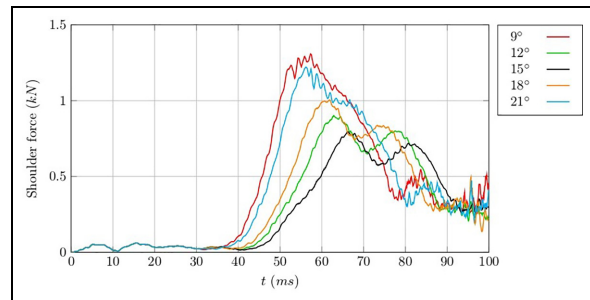

Figure 10. Set-up of the experimental impact tests.

Figure 11. Comparison between numerical and experimental results: dart force and panel acceleration in the time domain.

Figure 12. Low-wing aluminum configuration: shoulder force for all the angles.

Figure 13. Low-wing aluminum configuration: shoulder force for the angles of interest.

Figure 14. Low-wing aluminum configuration: lumbar force for all the angles.
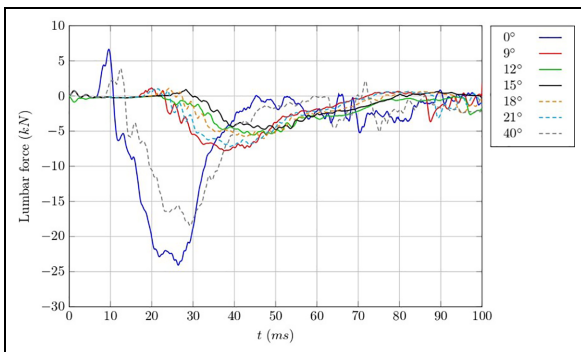

Figure 15. Low-wing aluminum configuration: lumbar force for the angles of interest.
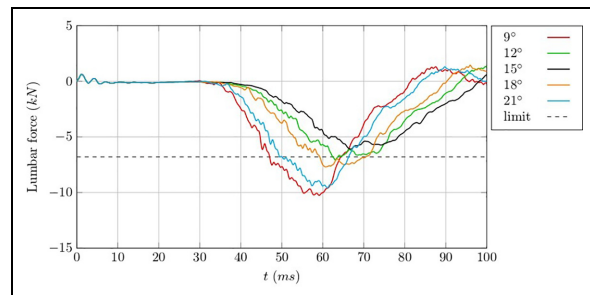

Figure 16. High-wing composite configuration: shoulder force for the angles of interest.

Figure 17. High-wing composite configuration: lumbar force for the angles of interest.

Regarding the composite aircraft, the shoulder loads shown in Figure 16 increased since the stiffness of the cabin is higher. For the lumbar loads in Figure 17, higher forces were reached compared to the aluminum configuration. Moreover, only the 15° case was below the limit. The range of angles which exhibit compliance with the regulation is lower. Therefore, the application of parachutes in composite aircraft must be properly evaluated. In addition, the impact angle tolerance must be increased by using other devices, such as shock-absorbing seats.

For the considered angles, a general trend of the impact dynamics has been observed: once happened the impact, the first contribution to the passenger is given by the shoulder belt. After that, the passenger is

withdrawn on the seat and then once again retained by the belt. Such a trend is clearly visible from the alternating of the peaks in Figures 16 and 17 themselves.

Finally, two optimal configurations for shoulder and lumbar forces can be compared. As can be seen in Figure 18, a first focus is performed on shoulder loads. The peak is larger for the composite configuration due to its higher stiffness. Since the lower part of the aluminum configuration is flat and the acceleration on impact is immediately transmitted to the occupants, the peak of the composite configuration is delayed compared to that of the metal one. On the other hand, the composite fuselage is curved, and it results in a very low acceleration transmission, until it
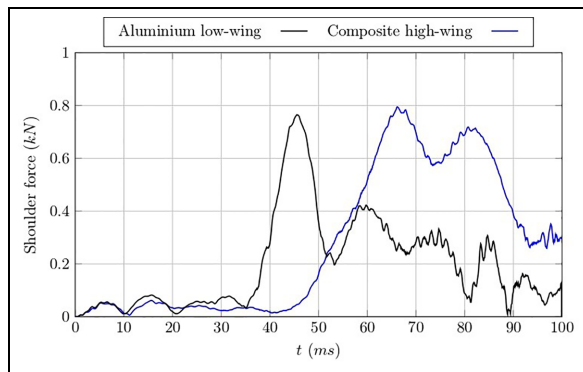
Figure 18. Low-wing metallic and high-wing composite configurations comparison: shoulder loads at the optimal impact angle.
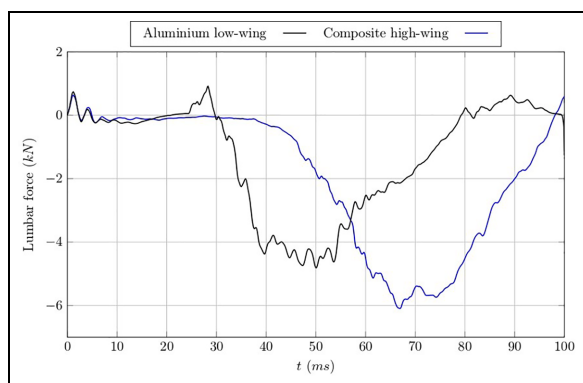
Figure 19. Low-wing metallic and high-wing composite configurations comparison: lumbar loads at the optimal impact angle.

reaches the two beams connecting the fuselage and the seat, corresponding to the two peaks shown in the graph.

Concerning lumbar loads, as shown in Figure 19, the composite configuration is the one reaching a higher peak due to its larger stiffness. In addition, as already noticed for shoulder loads, a time delay is due to the configuration of the bottom part of the cabin. Moreover, since the requirement limits are very close, further precautions for composite aircraft are needed.

Conclusions

This article defines the parachute emergency landing problem and the current state-of-the-art on the topic. Attention was paid to the loads transferred to the occupants in two GA aircraft configurations: a low-wing one made of aluminum alloy and a high-wing composite one. An experimental campaign of low-velocity impact tests was performed to define the constitutive model for the material adopted when dealing with composite configuration. A very good correspondence was obtained between the experimental and numerical results. Consequently, the latter was

deployed to correctly define the material card of the fuselage for the composite configuration, which was compared to the aluminum one. Both the FE models were defined using the LS-Dyna software. A parametric analysis to find the optimal impact angle for occupant safety was performed. The angle of incidence is an important design indication to better set the parachute ropes. Lumbar and shoulder loads analysis confirmed compliance with CS-23 requirement. This work demonstrates the possibility of adding the parachute also to the composite light aircraft configuration and how the Certification by Analysis approach can be extended to such a special condition as an emergency landing when the parachute deployment is verified. The analysis revealed higher shoulder and lumbar loads and a very small margin associated with limitations in the latter case. Therefore, the equipment of a composite aircraft with a parachute system must be properly evaluated and additional devices should be accounted.

Declaration of conflicting interests

The author(s) declared no potential conflicts of interest with respect to the research, authorship, and/or publication of this article.

Funding

ORCID iDs

Gennaro Di Mauro (iD) https://orcid.org/0000-0002-1949-4173
Michele Guida (iD) https://orcid.org/0000-0002-4116-5624

References

1. Saxena S. *Whole plane parachutes: towards safer aviation*. New Delhi: NISCAIR-CSIR, 2011, pp.30–31.
2. Maydew RC, Peterson CW and Orlik-Rueckemann KJ. *Design and testing of high-performance parachutes (la conception et les essais des parachutes a hautes performances)*. Neuilly-Sur-Seine: Advisory Group for Aerospace Research and Development, 1991.
3. NTSB. *Review of U.S. Civil Aviation Accidents, calendar year 2011*. Report No.: NTSB/ARA-14/01, 2014. Washington, DC: National Transportation Safety Board (NTSB).
4. Veronneau SJ and Ricaurte EM. *Aircraft accidents: investigation and prevention*. Philadelphia, PA: Fundamentals of aerospace medicine, 2008. pp.560–566.
5. Wiegmann DA and Taneja N. Analysis of injuries among pilots involved in fatal general aviation airplane accidents. *Accid Anal Prev* 2003; 35(4): 571–577.
6. NTSB. *Safety report, general aviation crashworthiness project: phase two – impact severity and potential injury prevention in general aviation accidents*. Report No.: NTSB/SR-85/01, 1985. Washington, DC: National Transportation Safety Board (NTSB).

7. Alaziz M, Stolfi A and Olson DM. Cirrus airframe parachute system and odds of a fatal accident in Cirrus aircraft crashes. *Aerosp Med Hum Perform* 2017; 88(6): 556–564.

8. Thomas R and Thomas D. Design analysis of an aircraft parachute recovery system for very light jets. In: *The 26th Congress of ICAS and 8th AIAA ATIO*, 2008.

9. Yeakle J, Lingard J, Underwood J, et al. Computer simulation of a whole-aircraft parachute recovery system. In: *The 20th AIAA aerodynamic decelerator systems technology conference and seminar, 2009*.

10. Overend S, Underwood J and Yeakle J. Testing of a two-stage reefed 27m polyconical parachute for the Cirrus Jet. In: *The 21st AIAA aerodynamic decelerator systems technology conference and seminar*, 2011.

11. Winter SR, Fanjoy RO, Lu CT, et al. Decision to use an airframe parachute in a flight training environment. *J Aviat Technol Eng* 2014; 3(2): 28.

12. Knacke TW. *Parachute recovery systems design manual*. China Lake, CA: Naval Weapons Center, 1991.

13. EASA. *Certification specifications for normal, utility, aerobatic and commuter category Aeroplanes CS-23*. European Aviation Safety Agency, Cologne, 2003.

14. Kindervater CM and Georgi H. Composite strength and energy absorption as an aspect of structural crash resistance. In: N Jones and T Wierzbicki. (eds) *Structural crashworthiness and failure*. Boca Raton, FL: CRC Press, 1993, pp.189–235.

15. Guida M, Lamanna G, Marulo F, et al. Review on the design of an aircraft crashworthy passenger seat. *Prog Aerosp Sci* 2022; 129: 100785.

16. Tita V, de Carvalho J and Vandepitte D. Failure analysis of low velocity impact on thin composite laminates: Experimental and numerical approaches. *Compos Struct* 2008; 83(4): 413–428.

17. Guida M, Marulo F, Belkhelfa FZ, et al. A review of the bird impact process and validation of the SPH impact model for aircraft structures. *Prog Aerosp Sci* 2022; 129: 100787.

18. Cairns DS and Lagace PA. A consistent engineering methodology for the treatment of impact in composite materials. *J Reinf Plast Compos* 1992; 11(4): 395–412.

19. Haug E and De Rouvray A. Crash response of composite structures. In: N Jones and T Wierzbicki. (eds) *Structural crashworthiness and failure*. Boca Raton, FL: CRC Press, 1993, pp.237–294.

20. Vicente JLS, Beltran F and Martìа nez F. Simulation of impact on composite fuselage structures. In: *Proceedings of THE European congress on computational methods in applied sciences and engineering (ECCOMAS)*, Barcelona, 2000.

21. Kindervater CM, Johnsson AF, Kohlgrüber D, et al. Crash and impact simulation of aircraft structures-hybrid and FE based approaches. In: *Proceedings of the European congress on computational methods in applied sciences and engineering (ECCOMAS)*, Barcelona, 2000.

22. Kostopoulos V, Markopoulos YP, Giannopoulos G, et al. Finite element analysis of impact damage response of composite motorcycle safety helmets. *Composites B* 2002; 33: 99–107.

23. Belingardi G, Gugliotta A and Vadori R. Fragmentation of composite material plates submitted to impact loading: comparison between numerical and experimental results. *Key Eng Mater* 1998; 144: 75–88.

24. Gottesman T and Girshovich S. Impact damage assessment and mechanical degradation of composites. *Key Eng Mater* 1998; 141-143(1): 3–18.

25. De Morais WA, Monteiro SN and d'Almeida JRM. Evaluation of repeated low energy impact damage in carbon–epoxy composite materials. *Compos Struct* 2005; 67: 307–315.

26. Naik NK and Shrirao P. Composite structures under ballistic impact. *Compos Struct* 2004; 66: 579–590.

27. Collombet F, Lalbin X and Lataillade JL. Damage prediction of laminated composites under heavy mass-low velocity impact. *Key Eng Mater* 1998; 141-143(1): 743–776.

28. Mikkor KM, Thomson RS, Herszberg I, et al. Finite element modelling of impact on preloaded composite panels. *Compos Struct* 2006; 75: 501–513.

29. Mamalis AG, Manolakos DE, Ioannidis MB, et al. The static and dynamic axial collapse of CFRP square tubes: finite element modelling. *Compos Struct* 2006; 74: 213–225.

30. Zhao GP and Cho CD. Damage initiation and propagation in composite shells subjected to impact. *Compos Struct* 2007; 78: 91–100.

31. Farley GL and Jones RM. Prediction of the energy-absorption capability of composite tubes. *J Compos Mater* 1992; 26(3): 388–404.

32. Lopresto V and Caprino G. Elastic response of circular CFRP plates under low-velocity impact. In: *Proceedings of The European conference on composite materials (ECCM)*, Brugge, 2002.

33. Kim JS and Chung SK. A study on the low-velocity impact response of laminates for composite railway bodyshells. *Compos Struct* 2007; 77: 484–492.

34. Guida M. Validity and applicability of the scaling effects for low velocity impact on composite plates. *Materials* 2021; 14(19): 5884.

35. Cantwell WJ. *Impact damage in carbon fibre composites*. PhD Thesis, University of London, London, 1985.

36. Broutman LJ and Rotem A. *Impact strength and toughness of fibre composite materials*. American Society for Testing and Materials (ASTM). West Conshohocken, 1975, pp.114–133.

37. Caputo F, Lamanna G, Perfetto D, et al. Experimental and numerical crashworthiness study of a full-scale composite fuselage section. *AIAA J* 2021; 59(2): 700–718.

38. Perfetto D, Lamanna G, Manzo M, et al. Numerical and experimental investigation on the energy absorption capability of a full-scale composite fuselage section. *Key Eng Mater* 2020; 827: 19–24.

39. Russo P, Guida M, Marulo F, et al. Analysis of integrated fuselage composite seat for small aircraft in crashworthiness applications. *J Mater Eng Perform* 2019; 28(8): 4856–4862.

40. Abrate S. *Impact on composite structures*. Cambridge: Cambridge University Press, 1998.

41. Choi HI and Chang FK. A model for predicting damage in graphite/epoxy laminated composites resulting from low-velocity point impact. *J Compos Mater* 1992; 26(14): 2134–2169.

42. Belingardi G, Gugliotta A and Vadori R. Numerical simulation of fragmentation of composite material plates due to impact. *Int J Impact Eng* 1998; 21(5): 335–347.

43. Belingardi G and Vadori R. Low velocity impact tests of laminate glass-fiber-epoxy matrix composite material plates. *Int J Impact Eng* 2002; 27(2): 213–229.
44. ASTM D7136: Standard test method for measuring the damage resistance of a fiber-reinforced polymer matrix composite to a drop-weight impact event. ASTM, 2007.

Appendix

Notation

Roman letters

E_i	Elastic modulus in i direction
G_{ij}	Shear modulus in ij direction
h	Ply thickness
S_C	Shear strength
t	Time
X_T	Longitudinal tensile strength
Y_C	Transverse compressive strength
Y_T	Transverse tensile strength

Greek letters

ε	Normal strain
ν_{ij}	Poisson Ratio in ij direction
ρ	Material density
σ	Normal stress

Acronyms

ASTM	American Society for Testing and Materials
BPRS	Ballistic Parachute Recovery Systems
BRS	Ballistic Recovery Systems
CAPS	Cirrus Airframe Parachute System
CS	Certification Specification
CF	Carbon Fiber
FAA	Federal Aviation Administration
FE	Finite Element
GA	General Aviation